Advanced microcopy to study tracking and spatiotemporal organization of intracellular membranes

Bertrand Cinquin, Alexandre Gidon, Anatole Chessel, Thierry Pecot, Jérôme Boulanger, Charles Gueudry, Charles Kervrann, Jean Salamero

▶ **To cite this version:**

Bertrand Cinquin, Alexandre Gidon, Anatole Chessel, Thierry Pecot, Jérôme Boulanger, et al.. Advanced microcopy to study tracking and spatiotemporal organization of intracellular membranes. Bio-Medical Materials and Engineering, 2011. inria-00541284

HAL Id: inria-00541284
https://inria.hal.science/inria-00541284

Submitted on 11 May 2011

HAL is a multi-disciplinary open access archive for the deposit and dissemination of scientific research documents, whether they are published or not. The documents may come from teaching and research institutions in France or abroad, or from public or private research centers.

L'archive ouverte pluridisciplinaire **HAL**, est destinée au dépôt et à la diffusion de documents scientifiques de niveau recherche, publiés ou non, émanant des établissements d'enseignement et de recherche français ou étrangers, des laboratoires publics ou privés.

Accepted in BBME

Advanced microscopy to study trafficking and spatiotemporal organization of intracellular membranes, at the single cell level

Bertrand Cinquin[1]*, Alexandre Gidon[1*], Anatole Chessel[1,2], Thierry Pécot[1,2,6], Jerome Boulanger[2,4], Charles Gueudry [2,5], Charles Kervrann[6] and Jean Salamero [1,2,3]

[1] UMR 144 CNRS-Institut Curie, [2] Cell and Tissue Imaging Facility IBiSA-Institut Curie, [3] Nikon Imaging Centre@Institut Curie-CNRS, Paris. [4]RICAM, Mathematical Imaging, Linz, Austria,[5] Roper Scientific SARL Evry, [6] INRIA Centre Rennes - Bretagne Atlantique.

Abstract :

The study of membrane plasticity and the role of molecular "machines" in the control of biogenesis of the endo-cellular membranes have highlighted the crucial role of the "Rab" GTPases family as organizing centers of functional molecular platforms in membrane sub-domains. Yet, to understand the regulation and coordination of these molecular assemblies, which are responsible for cellular dynamic architectures, a more global vision, the development and the correlation of approaches at different spatial and temporal scales are needed.

Focused biological models will be presented and will serve as guidelines that consider the mosaic of "Rabs domains" in particular at the plasma membrane within the context of recycling and exocytosis processes of fluorescently labeled cargos. In these *In Vivo* biological contexts, approaches aimed to measure and understand the multi-specific nature of these complexes have been developed. Our overall target is to model and assess the functional coordination between the different molecular machineries involved in the biogenesis of membrane sub-domains and their regulation. However, considering the "fickle" nature of such dynamic architectures, the current performance of image acquisition systems and the analytical tools at our disposal, many technological challenges must be overcome. Moreover, to extract maximum information on the same sample, the development of an adapted microscopy, correlating different modalities, is needed. Last but not least, accurate image descriptors, allowing automatic detection and classification of molecular behaviors in space and time, are indispensable.

Introduction:

While eukaryotic cells need to insure their integrity, they also have to communicate with their external medium. From yeast to human cells in tissues, mechanisms have been conserved through evolution that guarantee secretion, capture of diverse elements from the environment as well as recapture and shuttling of cellular receptors that allow selectivity of internalized molecules. Transferrin Receptor is a hallmark of constitutively endocytosed/recycling transmembrane receptors [1, 2]. Its expression and function is directly linked to cell division and accurate iron metabolism at the cellular level, through the endocytosis and processing of extracellular iron charged transferrin [3]. Central in ensuring that cargoes such as TfR/Tf complexes are delivered to their correct destinations within the cell are the Rab GTPases, proteins belonging to the Ras-like small GTP-binding protein superfamily. This large family of small GTPases which have emerged as master regulators of cellular membrane transport, controls membrane identity and vesicle budding, uncoating, motility and fusion through the recruitment of dedicated effector proteins [4]. Those effectors are diverse and may be sorting adaptors, tethering factors, kinases, phosphatases or motors acting at the different steps of membrane trafficking. Crosstalk between multiple Rab GTPases through shared effectors, or through effectors that recruit selective Rab activators, ensures the spatiotemporal regulation of vesicle traffic. We previously shown that stability, physiological localization and intracellular pathways of Langerin, a C type Lectin receptor almost exclusively expressed in Langerhans cell of the epidermis and

* Both authors contributed equally to this work

constitutively endocytosed and recycled to the plasma membrane, are under the strict control of active Rab11a on the membranes of the ERC. In strong contrast to the canonically used Transferrin Receptor recycling transmembrane protein, trafficking of Langerin is poorly affected by siRNA knock down of the Rab11a interacting RCP protein, while being totally miss-routed toward the lysosomal degradative pathway in the absence of an active Rab11a on the endosomal membranes [5]. Based on these strong evidences we now decided to decipher the dynamics processes of the latest steps of Rab11a dependant recycling pathway, using both Langerin and TfR as specific reporter molecules.

To get deeper insights in the dynamics of proteins, recycling from intracellular membrane pools to the plasma membrane, relatively new optical techniques have been thoroughly used over the last decades, that took advantages of fluorescent protein engineering. Total Internal Reflexion Fluorescence microscopy (TIRFM) based on the properties of evanescent waves propagation at the interface between two media with sufficiently different refractive indexes, is certainly the method of choice. TIRF microscopy allows for the imaging of a very thin layer near the cell surface, at about 100 or 200 nm depth from a glass cell support. The dynamic studies of events that occur between the cell and the external medium, is then possible. They may correspond to the entry (endocytosis) of extracellular species via the interaction with transmembrane protein or to the release of internal proteins devoted to secretion or plasma membrane location. Fusion of an individual intracellular vesicle to the PM is seen in TIRFM as a sudden appearing spot followed usually by a more or less slower decrease in fluorescence intensity. However fast-TIRF microscopy shows that as many as hundreds of such events may occur every minutes at different places within the surface of one cell. Moreover, it is almost impossible at a glance to assess the degree of temporal and spatial homogeneity of these events. Quantification of the large datasets generated is becoming a major obstacle. Manual tracking of cellular traffic is labor-intensive and observer-biased, and the variance within and between observers can influence results and eventually the conclusions. If one wishes to study multiple conditions at the single cell level, yet overcoming the basic limitation of pure qualitative or manual approaches, automatic image analysis of heavy image series is required that will allow statistical studies. In this work, our focus is the systematic study of the recycling mechanisms of transmembrane proteins.

Material and methods

Integrated imaging of single cell in Fast double TIRF-M

An integrated strategy toward HCS imaging of PM recycling of transmembrane receptors has been designed. As fast imaging as possible at an evanescent front is required. It should allow a global detection at the whole cell level. As more than one molecule have to be followed, simultaneous live cell imaging is necessary, at least for two fluorescent channels (typically, for GFP and mCh) need to be recorded. Our acquisition set-up is based on an inverted microscope equipped with a motorized TIRF arm (TE 2000, Nikon, SA). A laser bench providing AOTF controlled 488 nm and 561 nm wavelengths (Errol lasers) is interfaced and TIRF illumination performed through a 100x, NA 1.49 objective (CFI Plan Apo VC, Nikon, SA). Simultaneous double channel image acquisition is done using the ET-GFP/mCherry Chroma block filter completed with a dual view image splitter (Roperscientific, S.A.) in front of an EM-CCD (QuantEM, Roperscientific, S.A.). The whole stage is encaged, temperature, gas and humidity controlled (LIS, Switzerland). The Metamorph software (MDS, USA) is used as a driving interface. Sequence acquisitions were performed in as standardized as possible parameters of image capture. All data presented here and used to constitute our data base were obtained in stream mode, and display 1 frame/0.1s for about a minute duration. All sequences are then constituted of 600 images. Last but not least, live cells are physically constrained using home-made micro-patterning [6] allowing cell shape and size averaging as well as standardization of internal organization, through all individual experiments and further single cell studies.

Data analysis and mining

A new patch-based statistical change detection method previously developed (PBED software, licensing in progress; [7] and Boulanger et al., submitted to PLoS) is integrated as a first step in a workflow of image processing. Briefly, it is dedicated to extract all the individual endocytic or recycling events from a fast-TIRFM sequence by distinguishing them from lateral motions (vesicular trafficking). The latter are seen as suddenly appearing bright spots by comparing couples of images. Second, once detected, the PM docked recycling vesicle is supposed immobile and the third step is the computation, for each detected event, of a normalized temporal profile using another imaging development [8] (Hullkground AAP N°A1111356778943) that allows future study and comparison. The rational of our approach is further illustrated and commented within Figure 1.

Biological models

Melanome derived M10 cell stably expressing Langerin tagged with YFP in the luminal domain (M10+YFP) were cultivated as previously described [6]. M10 cells stably expressing Langerin tagged with YFP and Rab11a tagged with mCherry were then derived, isolated and cultivated with standard RPMI complete medium supplemented with Hygromycin. TfR-pHluorin plasmid was kindly provided by Dr D. Perrais [9] and also introduced in M10 cells.

Results

A Tfr/langerin

Our previous studies showed that Langerin and TfR do not respond similarly after silencing Rab11 proteins within M10 cells, Langerin overall trafficking and stability within the endocytic-recycling pathway being under the strict control of this Rab protein. In order to focus precisely on the late stage of recycling events, we used our automatic approach for spot detection PBED software on TIRFM 2D+t sequences. One important aspect to obtain reproducible results was to find a way to normalized all experimental data, which here means, standard image acquisition protocols, averaged size and shape of the cells and no need for further time consuming image treatment such as image registration, which could be necessary if biological samples were moving within the time series. The two latter issues were efficiently addressed using cell micro-patterning, following an approach described before (figure 1A) [6]. In figure 2A the PBED detection (green circles) is shown only on a part of the whole sequences (50 frames/600 frames) of two typical cells expressing either YFP-Langerine (left) or TfR-Phluorin (right) and was restricted to fast appearance detection. As illustrated in figure 2B and following the whole process described in figure 1 for data mining, all Langerine vesicles (left graph) suddenly appearing do not behave as the majority of the TfR vesicles (right graph). A first step of dynamic behavior classification (using Hausdorff distance) is presented where all detected fast appearing Langerine spots and thus 1D+t normalized curves were compared. Manual control was still used to sort and exclude very unusual behaviors such as the few extremely slow curves in figure 2 B (left panel). Finally we made the assumption that TfR dynamics recorded and analyzed under identical conditions describe a “standard behavior” for recycling receptors. Each normalized curves is linked to the corresponding raw data set within the whole patch data basis of detected events, allowing the expert to easily verifies and analyzes reasons of discrepancy, to analyze other image parameters, or to reconstitute 2D+time representations. The presented data (figure 2B, lower panel) statistically indicate at least two kinetics groups for Langerine spot behaviors, as compared to TfR vesicles.

B Langerine/Rab11a

As already mentioned, Langerine traffic is under the strict control of Rab11 [5]. In order to investigate the relationship between these two molecules at the very late stage of langerine vesicles recycling, we used simultaneous dual TIRFM. Imaging was done on micro-patterned M10 cells stably double

transfected for Langerine (YFP) and Rab11A (mCherry). We first assessed that both molecules are colocalized on structures moving near the plasma membrane (Fig. 3). Interestingly, while the Maximum Intensiy Projection map (M.I.P.) of the time series (Fig 3C) clearly showed both molecules being detected on identical moving structures (Arrow), an unexpected time delay (1 to few seconds, see thumbnails in Fig. 3B) between appearing red structures stabilized at one site of the plasma membrane and the appearance of bright spots of Langerin in the green channel, was almost systematically observed. In order to statistically analyze this particular behavior, PBED detection of 5 different cells was used on the Langerin channel part. Signals extracted from detections were submitted to the computational process described above. All 1D+t green signals detected within 600 frame series were then realigned and serve as a backbone for double color detection (245 on 479 detection in green channel) and analysis, with a minimum of 100 frames being recorded after green channel detection. Only events from the beginning of Rab11A structure appearance to the end of Langerin vesicles detection in particular spatial and temporal patches, were here considered for analysis. Method and numbers are presented in the Figure 3 legend. Both normalized and averaged red curve and clouds of dots confirmed a delay between Red spot (Rab11A) positioning in particular sites at which the bright signal was suddenly detected in the green channel (langerin) (Fig. 3D). In contrast, the overall kinetics of local fluorescence decline, once Langerine signals had peaked, was similar for both Red and Green fluorescent protein. Deeper investigations on this unexpected result are now undergoing, using classification approaches such as the one described in figure 2.

Discussion

TIRFM, by focusing on the cellular membrane, allows for the precise study of endocytosis/recycling and exocytosis pathways. The present work, proposes a framework for acquisition, detection and representation of individual recycling events, including cell averaging using new extracellular matrix based micropatterns and a novel statistical detection algorithm. Comparison of TfR and Langerin, two cargoes characterized as recycling transmembrane receptors, was used as a first case study. Among biological questions, this automated strategy enables us to distinguish different behaviors between TfR and Langerine transport intermediates, especially their relative lifetimes at specialized sites of their “docking/ fusion” at the plasma membrane. While the biophysical meaning of this divergence remains elusive so far, only computerized methods such as the one described in this paper allow for its finding and statistical analysis. Data mass extraction, molecular and others physical or chemical perturbations, should now help us in deciphering the mechanisms underlying different temporal molecular comportments of a process that should be at the most, similar.
In this respect, we now made use of dual-color TIRFM to compare the spatiotemporal dynamics of a recycling transmembrane protein along with others proteins that constitute the complex machinery of the cell involved in the molecular mechanisms of the basic processes of recycling, docking and fusion of vesicles at the plasma membrane. An image data base, constituted of automatically detected events, was used together with a pipeline of normalization and visualization approaches to extract a first series of results. Here was presented a time correlated study of Rab11a dynamics and late events of Langerine recycling. A number of unexpected and informative elements came to light, among them, the time-delay between a rab11A positive carrier vesicle appearing and stabilizing at a spatially defined site at or very close to the cell surface and the beginning of fusion identified as the release of the Langerine in the plane of the PM. Such parameters are now easily statistically measured. Taken together with other studies in the literature [8] showing that components of the exocyst docking complex, such a Sec6, Sec8, Sec15 or Exo70 , colocalize with Rab11 on endosomal membranes, our data strengthen the involvement of Rab11a complexes or domains [4, 10], not only in the biogenesis and maintenance of the endosomal recycling compartment (ERC), but also in the very late stage of membrane cargo delivery at the PM. Dynamic aspects of perspectives described above still require conceptual developments, for instance, in the field of microscopy imaging dealing with toxicity, speed or time regimes for instance [11].

References :

(1) ***Bleil J.D. and Bretscher M.S.*** *Transferrin receptor and its recycling in hela cells. EMBO J.1982 (1) 351–355.*

(2) ***B.D. Grant and J.G. Donaldson****, "Pathways and mechanisms of endocytic recycling, Nat. Rev. Mol. Cell. Biol.2009 (10) 597–560.*

(3) ***Mllner E.W., Neupert B., and Kuhn L.C.*** *A specific mRNA binding factor regulates the iron-dependent stability of cytoplasmic transferrin receptor mRNA. Cell. 1989 (58) 376–382.*

(4) ***Stenmark H.*** *Rab GTPases as coordinators of vesicle traffic. Nat Rev Mol Cell Biol. 2009 10(8) 513-525.*

(5) ***Uzan-Gafsou S, Bausinger H, Proamer F, Monier S, Lipsker D, Cazenave JP, Goud B, de la Salle H, Hanau D and Salamero J.*** *Rab11A controls the biogenesis of Birbeck granules by regulating Langerin recycling and stability. Mol Biol Cell. 2007 (8):3169-79.*

(6) ***Théry M, Racine V, Pépin A, Piel M, Chen Y, Sibarita JB, and Bornens M.*** *The extracellular matrix guides the orientation of the cell division axis. Nat Cell Biol. 2005 (10)947-953.*

(7) ***Pécot T, Kervrann C, Bardin S, Goud B and Salamero J.*** *Patch-based Markov models for event detection in fluorescence bioimaging. Med Image Comput Comput Assist Interv Int Conf Med Image Comput Comput Assist Interv. 2008 11(Pt 2) 95-103.*

(8) ***Chessel A, Cinquin B, Bardin S, Salamero J, and Kervrann C*** *. Computational geometry for convexity based geometrical scale-spaces and modal decompositions. Applications to light microscopy video imaging. SSVM 2009, in Lecture Notes in Computer Science (LNCS) 2009 (5567) 770-781.*

(9) ***Merrifield C.J., Perrais D., and Zenisek D.****. Coupling between clathrin-coated-pit invagination, cortactin recruitment, and membrane scission observed in live cells. Cell. 2005 (121) 593–606.*

(10) ***Wu S, Mehta SQ, Pichaud F, Bellen HJ,and Quiocho FA.*** *Sec15 interacts with Rab11 via a novel domain and affects Rab11 localization in vivo. Nat Struct Mol Biol. 2005 (10) 879-85.*

(11) ***Boulanger, J., Kervrann C., Elbau P., Bouthemy P., Sibarita J.B. and Salamero J.*** *Patch-based non-local functional for denoising fluorescence microscopy image sequences. IEEE Transactions on Medical Imaging. 2010 (29) 442-454.*

Figure legends :

Figure 1 : Rational of single cell imaging and analysis pipeline for recycling (or secretory) events data mining

Maximum Intensity projections of raw TIRFM sequences of two cells (top and bottom part) attached to micro-patterns (here a crossbow shaped micro-pattern). Both cells were recorded for 1 min at 100ms/f simultaneously in two fluorescent channels (Red channel on the left part and green channel on the right part). B) Projection of a Langerin-YFP dynamics sequence (600 frames) in a M10 cell by TIRFM. Green and red circles correspond to sudden appearances and disappearances as they are automatically detected and selected using the Patch Based Event Detection software, respectively. Yellow circles correspond to the overlay of "on and off" detections. They mostly correspond to vesicles suddenly appearing at the plasma membrane that further quickly vanish within the evanescent wave front. C) Two temporal curves illustrating two different behaviors of automatically detected events. Intensity versus time graphics are plotted from raw signals in the sequence of the events indicated in the image thumbnails. On the left side, one particular event showing both fast appearance and disappearance at the same spatial location. On the right side, a detected fast appearance is followed by slower vanishing of the signal within the same local space. D) Multiple 1D+t representations of spot detection and behavior by PBED at the single cell level, showing the large numbers of events, their heterogeneity in intensity and duration. E) Decomposed graphic showing the result of our computation of such individual events. Beginning of the detected event (horizontal arrow) is based on automatic detection of maximum intensity over time, in each spots previously detected by PBED. scale space is used to compute the end of the event (vertical arrow). Normalization is taking observational photobleaching into account. Final step is the extraction of the convex hulls in each temporal sequence of detected spots. In red the final normalized decrease fit used for analysis.

Figure 2 : Computation of temporal fluorescence decreases of recycling and fusing TfR or Langerin vesicles at the single cell level.

A) Detection of langerin (left) and TfR (Right) of only appearing spots is shown. TIRF maximum intensity projections of only 50 frames among 600 are shown on the images. Manual validation was performed in parallel on these small series showing less than 10% discrepancy between automated and visual detections. B) Curves of fluorescence declines were computed as described in Figure 1 for each detected spots of fast appearing vesicles. All the normalized decreases of the detected spots for one Langerin-YFP (left) and one TfR-pHl (right) TIRFM sequences on micro-patterned single cells are plotted. Classification of slow (blue) versus fast (red) fluorescence decrease is performed by calculating Haustdorf distances on one particular sequences of Langerin-YFP cell.

Figure 3 : Computation of temporal behaviors of double fluorescence recycling vesicles docking and fusing with the plasma membrane at the single cell level

Double TIRFM image of M10 cells, stably transfected for both Langerine-YFP (Green) and Rab11A-mCh (Red) adherent to a crossbow micropattern (image representing one frame over 600 at 10 fps). Scale bar is 5mm. B) Thumbnails with indicated numbers of frame, taken from series of images in the area indicated in C. Note that color overlay (yellow) are regularly detected, within small area, yet being very transient. C) Maximum intensity Projection of the whole sequence at the single cell level (from the cell in A; M.I.P. of 600 frames). Most of the dual color tracks are located at the periphery of the cell. The red channel image was shifted from one pixel (+1) to the top, in order to better view the coincidence of both Langerine and Rab11A signal trajectories, when they occur. D) Compilation of all events detected in the green channel within 5 different experiments, are computed as indicated in figure 2 using the PBED algorithm. We report the detection map made on Langerin side (Green), on the Rab11 side (Red). Curves of Langerin events have been normalised to 1 taking the nearest maximum peaks of intensity (Y axis) and the minimum in the one hundred frames after. All 1D+t green signals are realigned and plotted, accordingly. Then all 1D+t double colors signals are compared over the whole time series (taking into account the one hundred frames before. Events have to be complete, meaning from the beginning of Rab11 structures appearance until the Langerin disappearance. This is why incomplete double events are not included. Red 1D+t signals are realigned and plotted within the same sequences. Bleaching was corrected on the Rab11 average curve, by subtraction of a simple straight line. Coefficient was evaluated by considering the average of bleaching for the five experiments.

On five experiments, 479 events have been detected, 245 (51%) are double events but only 125 (26%) have been taken in account. Clouds of points represent all individual events for both labeling (n= 125) over time. Indicated averages are arithmetic (red and green plain lines).

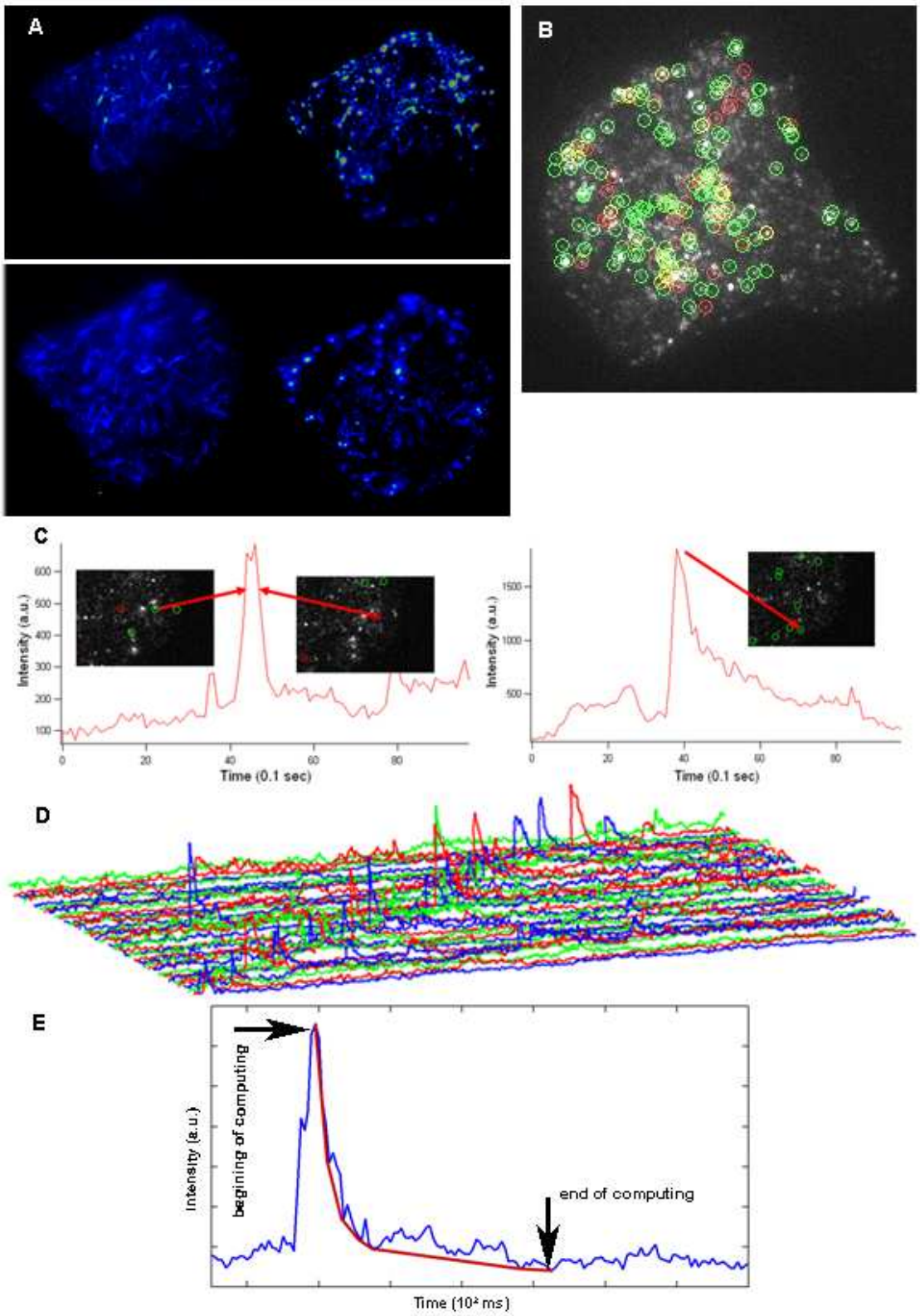
A
B
C
Intensity (a.u.)
Time (0.1 sec)
Intensity (a.u.)
Time (0.1 sec)
D
E
beginning of computing
end of computing
Intensity (a.u.)
Time (10² ms)

Figure 1

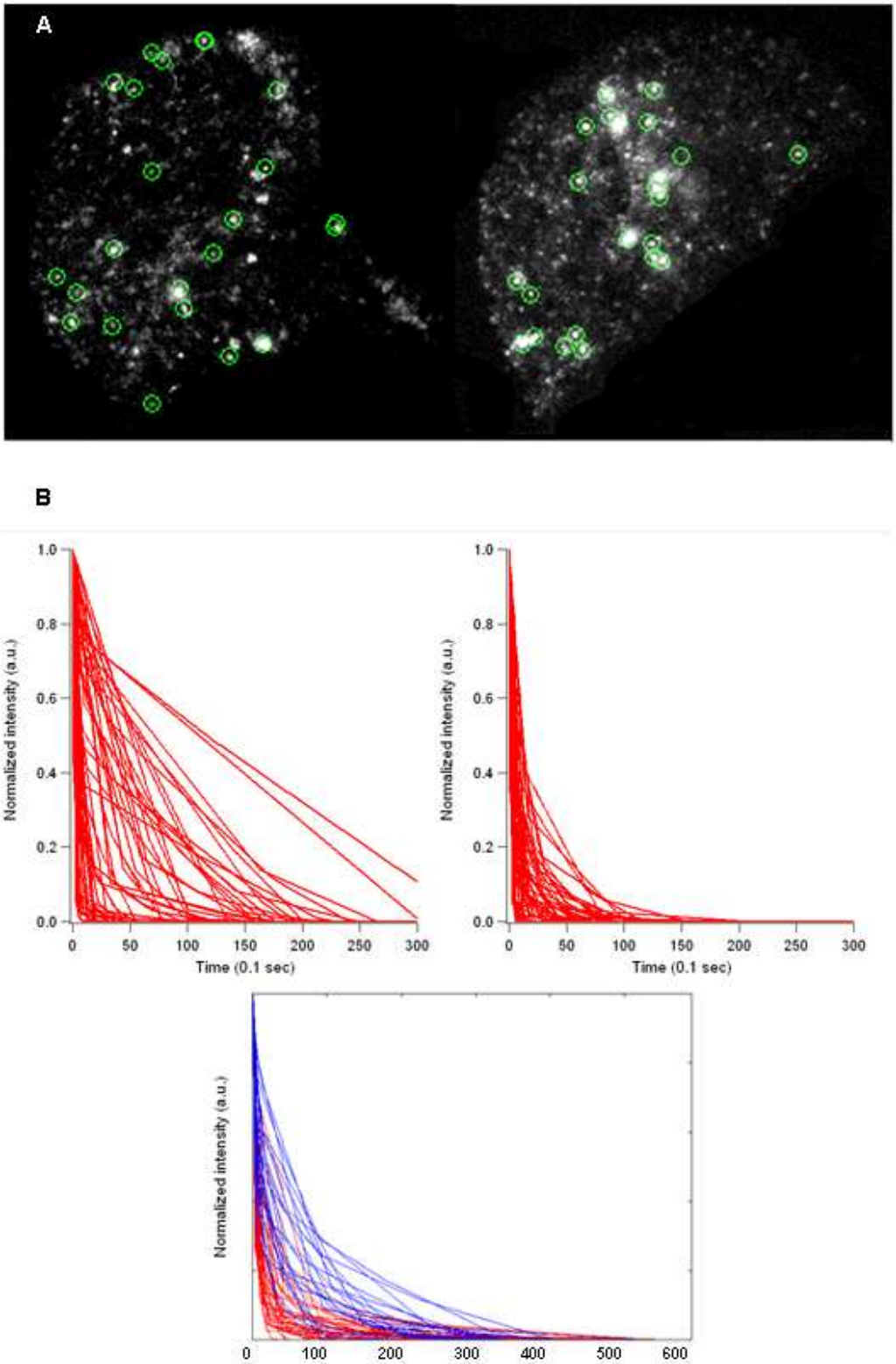
A
B
Normalized intensity (a.u.)
Time (0.1 sec)
Normalized intensity (a.u.)
Time (0.1 sec)
Normalized intensity (a.u.)

Figure 2

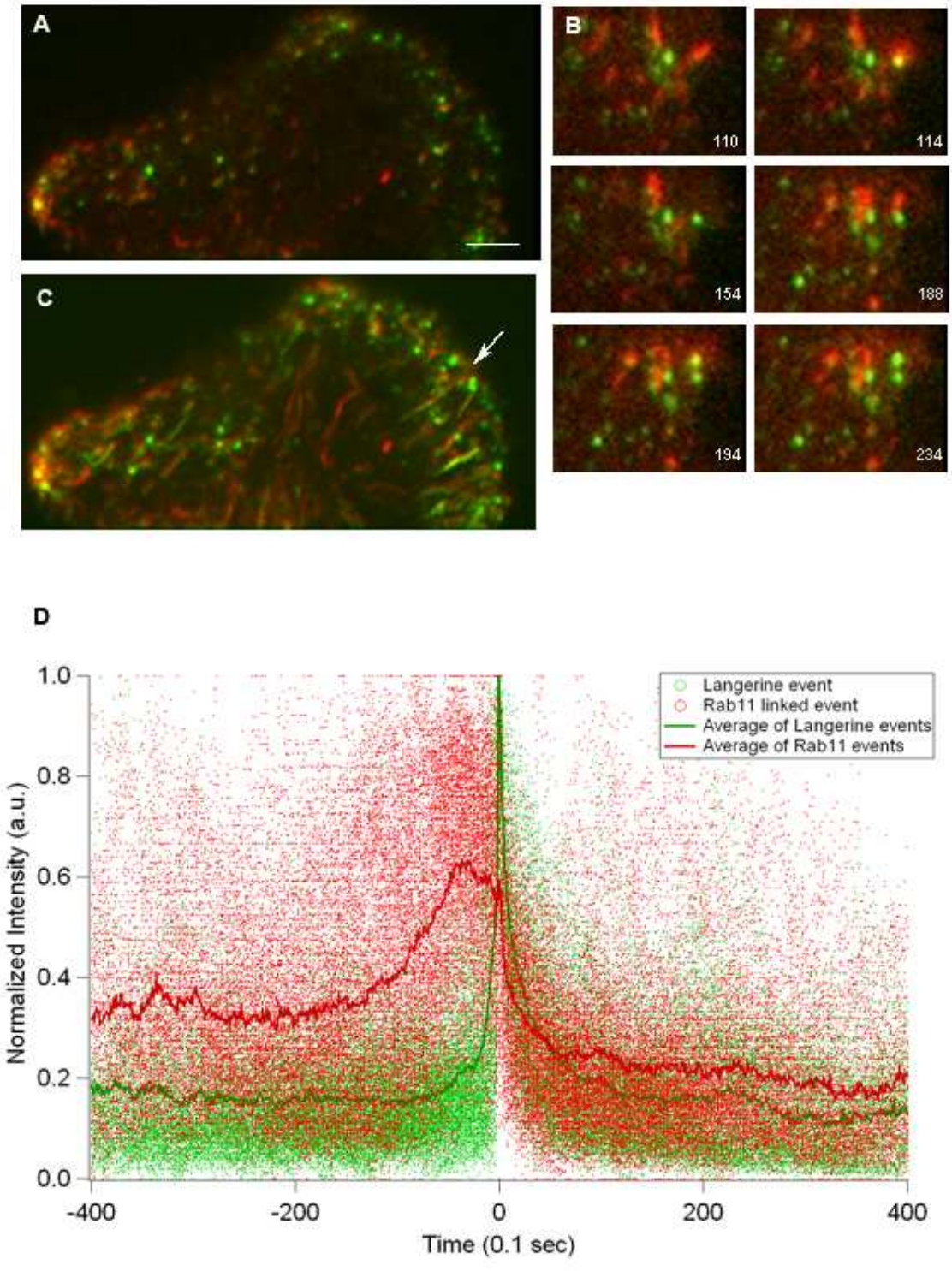
A
B
110
114
154
188
194
234
C
D
Langerine event
Rab11 linked event
Average of Langerine events
Average of Rab11 events
Normalized Intensity (a.u.)
1.0
0.8
0.6
0.4
0.2
0.0
-400
-200
0
200
400
Time (0.1 sec)

Figure 3